Neuroglobin attenuates β-amyloid neurotoxicity *in vitro* and transgenic Alzheimer phenotype *in vivo*

Adil A. Khan*, Xiao Ou Mao, Surita Banwait, Kunlin Jin, and David A. Greenberg

Buck Institute for Age Research, 8001 Redwood Boulevard, Novato, CA 94945

Edited by Solomon H. Snyder, Johns Hopkins University School of Medicine, Baltimore, MD, and approved October 3, 2007 (received for review June 29, 2007)

Neuroglobin (Ngb), a vertebrate globin expressed primarily in neurons, is induced by and protects against neuronal hypoxia and cerebral ischemia. To investigate the spectrum and mechanism of Ngb's neuroprotective action, we studied the effect of transgenic overexpression of Ngb on NMDA and β-amyloid (Aβ) toxicity in murine cortical neuron cultures *in vitro* and on the phenotype of Alzheimer's disease (AD) transgenic ($APP_{Sw,Ind}$) mice. Compared with cortical neuron cultures from wild-type mice, cultures from Ngb-overexpressing transgenic (Ngb-Tg mice) were resistant to the toxic effects of NMDA and Aβ(25–35), as measured by polarization of cell membrane lipid rafts, mitochondrial aggregation, lactate dehydrogenase release, and nuclear fragmentation. In addition, compared with $APP_{Sw,Ind}$ mice, double-transgenic (Ngb-Tg × $APP_{Sw,Ind}$) mice showed reductions in thioflavin-S-stained extracellular Aβ deposits, decreased levels of Aβ(1–40) and Aβ(1–42), and improved behavioral performance in a Y-maze test of spontaneous alternations. These findings suggest that the spectrum of Ngb's neuroprotective action extends beyond hypoxic–ischemic insults. Ngb may protect neurons from NMDA and Aβ toxicity by inhibiting the formation of a death-signaling membrane complex, and interventions that increase Ngb expression could have therapeutic application in AD and other neurodegenerative disorders.

globin | lipid raft | neurodegeneration | neuroprotection | NMDA

Neuroglobin (Ngb) is a vertebrate globin that is localized to neurons, binds O_2 and other gaseous messengers, is transcriptionally induced by hypoxia and ischemia, and protects against hypoxic neuronal death and ischemic brain injury (1). However, the mechanism through which Ngb exerts its neuroprotective effect is unclear. We found recently that hypoxia induces polarization of plasma membrane lipid microdomains (rafts) that appear to mediate hypoxic neuronal death because inhibiting their formation enhances survival of hypoxic neurons (A.A.K., unpublished data). Moreover, raft polarization precedes caspase activation and mitochondrial release of cytochrome *c*, indicating that it is an early—and, thus, potentially reversible—event in cell-death pathways. Neurons from Ngb-overexpressing transgenic (Ngb-Tg) mice (2, 3) do not undergo membrane polarization in response to hypoxia and are resistant to hypoxic cell death, suggesting that Ngb may protect neurons from hypoxia by interfering with this cell-death signaling complex.

In addition to its protective effects against neuronal hypoxia *in vitro* and cerebral ischemia *in vivo*, Ngb also reduces oxidative injury from H_2O_2 or paraquat (4) and β-amyloid (Aβ)-induced toxicity (5) in cultured neural cell lines. To determine whether inhibition of membrane polarization-dependent neuronal death by Ngb extends to insults other than hypoxia, we investigated the effect of transgenic overexpression of Ngb on the neuronal toxicity of the excitatory amino acid, NMDA, and the Alzheimer's disease (AD)-related peptide, Aβ. Compartmentalization by membrane microdomains has been speculated to be important in the processing of amyloid precursor protein (APP), from which Aβ is derived, and in regulating the access of APP to secretases involved in its cleavage (6, 7). In addition, inhibitors of the Rho GTPase Rac1, which is implicated in microdomain polarization of the plasma membrane, inhibit APP processing and Aβ production (8, 9).

Using progeny of crosses between Ngb-Tg mice (2, 3) and transgenic mice that express a mutant (K670N, M671L, V717F) form of human APP ($APP_{Sw,Ind}$) associated with familial AD (10), we show that Ngb overexpression inhibits AD-related raft aggregation and membrane polarization and associated neuronal death *in vitro*, and that $Ngb^{++}/APP_{Sw,Ind}$ mice produce reduced amounts of Aβ(1–40), Aβ(1–42), and amyloid plaques in the brain. These findings may have implications for the pathophysiology and treatment of AD.

Results

To investigate the commonality and physiological significance of cell membrane polarization and its inhibition during death signaling in neurons, we studied the effects of NMDA and Aβ in neuronal cultures from mouse cerebral cortex. Both 20 μM Aβ(25–35) (Fig. 1*a*) and 300 μM NMDA (Fig. 1*b*) induced rapid polarization of raft microdomains in cortical neurons, which was associated with aggregation of the mitochondrial network beneath the polarized raft complex. Aβ(35–25), which is not neurotoxic, had no such effect. Ngb-Tg neurons were protected from Aβ(25–35)- (Fig. 1 *c* and *d*), and NMDA- (Fig. 1*c*) induced death and did not undergo microdomain polarization or mitochondrial aggregation. The protective effect of Ngb overexpression against Aβ(25–35) was reversed by siRNA directed against Ngb (Fig. 1*e*). In contrast to the effect of 300 μM NMDA, exposure to 2 mM NMDA (which causes rapid, caspase-independent neuronal death) (11) caused neuronal death without spatial alignment of lipid rafts and the mitochondrial network and was not inhibited by Ngb overexpression (Fig. 1 *c* and *f*).

If interruption of plasma membrane polarization accounts for the protective effect of Ngb overexpression, other agents that block polarization should be similarly protective. To test this prediction, we treated cultures with mevastatin, which inhibits HMG-CoA reductase and interferes with cholesterol biosynthesis (12), or the cholesterol-extracting agent methyl-β-cyclodextrin (βCD), which depletes membrane cholesterol acutely and protects cortical neurons from NMDA toxicity (13). We reasoned that, by altering membrane composition, cholesterol depletion might interfere with the formation of death-signaling complexes. Depletion of neuronal plasma membrane cholesterol by either mevastatin or βCD inhibited microdomain polarization triggered by Aβ (Fig. 1 *g* and *h*) and NMDA and protected cortical neurons from Aβ- and NMDA-induced cell death (Fig. 1*i*). Addition of exogenous cholesterol restored

Author contributions: A.A.K., K.J., and D.A.G. designed research; A.A.K., X.O.M., S.B., and K.J. performed research; A.A.K., X.O.M., S.B., and D.A.G. analyzed data; and A.A.K. and D.A.G. wrote the paper.

The authors declare no conflict of interest.

This article is a PNAS Direct Submission.

*To whom correspondence should be addressed. E-mail: akhan@buckinstitute.org.

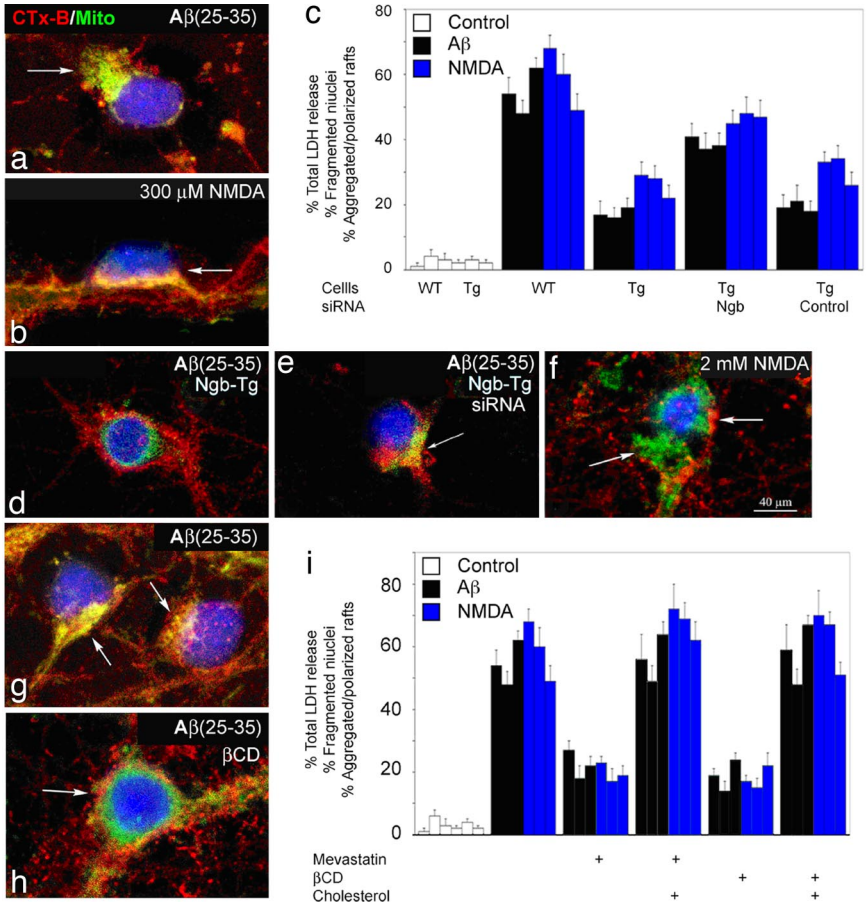

Fig. 1. Ngb overexpression and cholesterol depletion inhibit Aβ- and NMDA-induced membrane polarization and *in vitro* neurotoxicity. (*a*) Ten minutes after treatment with 20 μM Aβ(25–35), cultured cortical neurons from wild-type mice (9 DIV) show polarization (arrow) of cholera toxin B subunit (CTx-B) membrane staining (red) and associated mitochondrial aggregation (MitoFluor Green, green). (*b*) Membrane polarization and mitochondrial aggregation (arrow) also are seen 5 min after treatment with 300 μM NMDA and 5 μM glycine. (*c*) Neuronal cell death, measured by LDH release or fragmentation of DAPI-stained nuclei, and associated cell polarization (*Left*, *Middle*, and *Right* in each group of three bars) are increased 48 h after treatment with 20 μM Aβ(25–35) and 24 h after treatment for 10 min with 300 μM NMDA/5 μM glycine. These effects are attenuated in cultures from Ngb-Tg mice and restored in Ngb-Tg cultures preincubated for 24 h with 4 μM Ngb (but not control) siRNA. (*d* and *e*) Ngb-Tg neuron treated for 3 h with 20 μM Aβ(25–35) shows neither membrane polarization nor mitochondrial aggregation (*d*), which are restored (arrow) after preincubation for 24 h with 4 μM Ngb siRNA (*e*). (*f*) Treatment for 15 min with NMDA at a 2 mM concentration, which produces rapid cell death, fails to elicit membrane polarization or mitochondrial aggregation. The left arrow indicates mitochondria (green), and the right arrow indicates Ctx-B staining (red), which are not aligned. (*g* and *h*) Membrane polarization and mitochondrial aggregation induced by treatment with 20 μM Aβ(25–35) for 48 h (*g*) are prevented by pretreatment for 1 h with 1% βCD (*h*). Cholesterol depletion, produced by pretreatment with 300 nM mevastatin for 5 days or with 1% βCD for 1 h, reduces LDH release, nuclear fragmentation, and cell polarization, measured 48 h after treatment with 20 μM Aβ(25–35) and 24 h after treatment for 10 min with 300 μM NMDA/5 μM glycine. (*i*) The effects of mevastatin and βCD are reversed by coincubation of mevastatin-treated cultures with 5 μM cholesterol or by incubating βCD CD-treated cultures for 15 min with 2 mM cholesterol complexed with 2.5% βCD. Blue in photographs corresponds to DAPI-stained nuclei. Bars in graphs indicate mean values ± SEM from at least three experiments.

microdomain polarization and reversed the protective effects of mevastatin and βCD.

To investigate the effect of Ngb overexpression on AD pathophysiology *in vivo*, we crossed our Ngb-Tg mice with $APP_{Sw,Ind}$ mice, which deposit Aβ in AD-like amyloid plaques beginning at 8–10 months of age (10), to create $Ngb^{++}/APP_{Sw,Ind}$ double transgenics. In $APP_{Sw,Ind}$ mouse brains and AD patient brain sections, Aβ-positive extracellular plaques stain positively for CTx-B, suggesting that an association of Aβ with GM1 membrane microdomains is common to both human AD and mouse models of FAD (Figs. 2 and 3) in accord with several groups' observations (14, 15). Further, in $APP_{Sw,Ind}$ mice brains, Aβ and CTx-B are colocalized in aggregated GM1 microdomains on the somal surface of neurons (Fig. 3 *c*, *d–g*) in accord with prior observations (16). In many neurons, Ctx-B is internalized and colocalized with nuclear DAPI, reflecting active endocytosis after raft aggregation and somal polarization (Fig. 3 *h* and *i*).

Our results demonstrate that in $Ngb^{++}/APP_{Sw,Ind}$ brain neuronal somata down-regulate plasma membrane GM1, and APP and somal microdomains remain uniformly distributed throughout the soma (Fig. 4 *a–e*). An important event in the pathogenesis of AD is thought to be the assembly of Aβ(1–42) into fibrils and its deposition in β-sheet-rich thioflavin-S-positive structures (17). $Ngb^{++}/APP_{Sw,Ind}$ mice showed little thioflavin-S staining, compared with $APP_{Sw,Ind}$ littermate controls (Fig. 4 *f* and *g*), although APP levels were similar in both groups. Consistent with the absence of thioflavin-S staining in $Ngb^{++}/APP_{Sw,Ind}$ double transgenic mice, brain tissue from these mice, analyzed by immunohistochemistry and ELISA, showed decreased Aβ(1–40) and Aβ(1–42), compared with $APP_{Sw,Ind}$ littermate controls (Fig. 4*h*).

AD transgenic (including $APP_{Sw,Ind}$) mice exhibit a variety of neurobehavioral abnormalities that reflect impaired learning and memory (18, 19). These abnormalities include defects in spatial learning, which can be assessed by tests of spontaneous

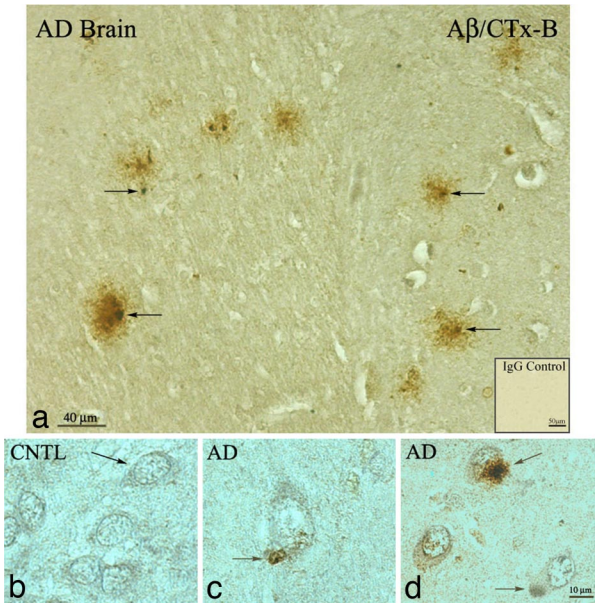

Fig. 2. $A\beta_{1-42}$ and CTx-B staining colocalize to amyloid plaques in AD brain neurons. (*a*) Light microscopy images of immunoperoxidase staining for $A\beta_{1-42}$ (mAb 3D6 brown) and CTx-B (nickel) in AD brain sections. (*Inset*) Control immunocytochemistry by using mouse and rabbit IgG showed no staining. (*b*) Nonpolarized CTx-B staining (nickel) and lack of $A\beta_{1-42}$ (brown) in neurons from control human brain sections. (*c*) Representative AD brain neuron with plaque developing from polarized somal microdomain (arrow). (*d*) Representative AD brain field with neuron with developing plaque (top arrow), neuron with polarized CTx-B staining (nickel) and colocalized onset of $A\beta_{1-42}$ production (brown) (arrow), and unaffected neuron. Similar staining results were obtained with a series of Aβ Abs (listed in *Methods*). The immunocytochemistry was repeated three times with similar results.

alternations in the choice of maze arms (20). We used a Y-maze to quantify spontaneous alternations in $Ngb^{++}/APP_{Sw,Ind}$ mice, compared with $APP_{Sw,Ind}$ littermate controls. We found that Ngb overexpression reversed the deficit observed in the latter (Fig. 4*i*), indicating that the beneficial effect of Ngb extended to behavioral alterations in $APP_{Sw,Ind}$ mice.

Discussion

We report two principal findings. First, transgenic overexpression of Ngb reduced the toxic effects of NMDA and Aβ, including membrane polarization, mitochondrial aggregation, and cell death, in cortical neuron cultures. This effect was abolished by Ngb siRNA, indicating its specificity, and was reproduced by cholesterol-depleting agents and restored by cholesterol, suggesting its dependence on membrane lipid composition. Second, overexpression of Ngb in AD transgenic ($APP_{Sw,Ind}$) mice resulted in a milder phenotype, which was characterized by a reduction of thioflavin-S-stained extracellular deposits, decreased levels of Aβ(1–40) and Aβ(1–42), and improved cognitive performance. Thus, Ngb appears to act by a polarized membrane-signaling complex to inhibit Aβ toxicity *in vitro* and attenuates the sequelae of APP mutations *in vivo*.

Ngb is a heme protein that is distantly related to myoglobin and hemoglobin and expressed primarily in neurons. In previous studies, we found that Ngb expression is induced by neuronal hypoxia or cerebral ischemia, and that Ngb reduces neuronal death in these settings, suggesting a role as an endogenous neuroprotectant (2, 21, 22). Although Ngb binds O_2, enhanced O_2 delivery is considered unlikely to explain its protective effect against hypoxic or ischemic injury because its intraneuronal concentration ($\approx$1 μM) is too low to account for appreciable changes in intracellular O_2 levels (1). In addition, Ngb appears to reduce neuronal death from other than hypoxic or ischemic insults (4, 5). Consequently, alternative protective mechanisms have been proposed, including scavenging of reactive oxygen or nitrogen species (23) and promoting the dissociation of G protein $\beta\gamma$ subunits (24) that activate antiapoptotic pathways (25). In addition, studies of protein–protein interactions have revealed Ngb-binding partners, providing further clues to its mode of action. For example, Ngb coimmunoprecipitates with the raft-associated membrane protein flotillin-1 (26), which suggested to us that Ngb might act by raft-associated membrane complexes that regulate cell death. Such death-inducing signaling complexes are observed in the immune system, where they appear to transduce Fas/CD95-mediated apoptosis (27).

We reported previously that Ngb-overexpressing transgenic mice are resistant to cerebral ischemia (2), and we used neuronal cultures prepared from these mice to investigate the cellular mechanisms that underlie protection from hypoxic-ischemic injury by Ngb (A.A.K., unpublished data). These studies demonstrated that protection by Ngb is associated with impaired function of a hypoxia-induced polarized cell membrane complex that is enriched in GM1 ganglioside, contains proteins that regulate ion transport (Kv2.1 K^+ channel, Na^+/K^+-ATPase β2 subunit, NCX1 Na^+/Ca^{2+} exchanger, and TRPC5 transient receptor potential cation channel), interacts with the actin cytoskeleton, and overlies sites of mitochondrial aggregation. In the present study, we found that membrane polarization and mitochondrial aggregation also are associated with NMDA- and Aβ-induced neuronal death and are inhibited by overexpression of Ngb.

The finding that Ngb not only blocks the toxic effects of Aβ, but also reduces Aβ levels, suggests that, in addition to acting downstream of Aβ, it also may interfere with Aβ production. The mechanisms that might be involved are unclear, but microdomain aggregation, APP processing, spatial segregation of secretases, and GM1 binding all point to an important role for membrane microdomains in the pathology of AD (6, 7, 14–16). We suggest that inhibition of membrane compartmentalization by Ngb retards raft aggregation signaling dynamics required for APP secretase processing and Aβ production. As such, APP processing is typical of several proteins whose processing depends on dynamic microdomain aggregation and endocytotic cycles. Disruption of microdomain and cytoskeletal aggregation by Ngb could affect Aβ production at several sites, although our data suggest that modulation of somal polarity and the spatial segregation of secretases (6, 7) may be involved. Our results demonstrate decreased plasma membrane GM1 in $Ngb^{++}/APP_{Sw,Ind}$ neurons and up-regulation of this ganglioside in the nucleus. GM1 is a major constituent of membrane microdomains, and GM1 microdomain aggregation has been implicated in the amyloidogenic processing of APP. Further, Aβ binding to GM1 may act as a seed for the conversion of monomeric, nontoxic Aβ to its toxic aggregated fibrillar form (28). The down-regulation of plasma membrane GM1 in $Ngb^{++}/APP_{Sw,Ind}$ mice may, therefore, regulate membrane microdomain signaling and inhibit Aβ production *in vivo*.

Polarized membrane death signaling may represent a therapeutic target in acute and chronic neurodegeneration. In fact, the ability of cholesterol-depleting drugs to reduce levels of Aβ40 and Aβ42 *in vitro* and *in vivo* (29), protect against excitotoxic (13) and Aβ-induced (30) neurotoxicity *in vitro*, and reduce the risk of clinical stroke and AD (31) might operate through such a mechanism. By extension, measures that increase Ngb expression could have beneficial effects in a range of neurological disorders.

Methods

Mice. Ngb-Tg mice were generated as described previously (2, 3). $Ngb^{++}/APP_{Sw,Ind}$ transgenic mice were produced by crossing homozygous Ngb^{++} transgenic mice (FVB $\times$ CD1) with heterozygous

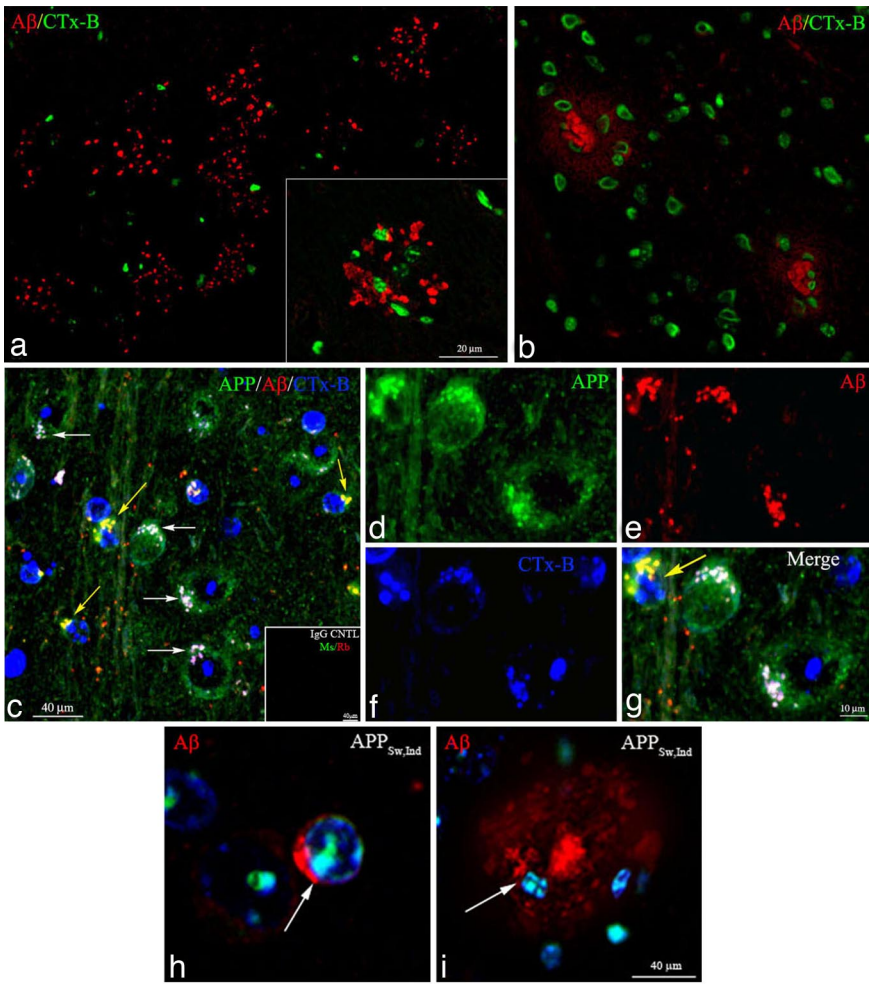

Fig. 3. Localization and polarized topographical distribution of CTx-B, hAPP, and Aβ as shown by immunocytochemistry in $APP_{Sw,Ind}$ mice brain neurons. $APP_{Sw,Ind}$ brain sections were stained with combinations of CTx-B (blue), anti-APP (CT15) (green), and anti-Aβ(3D6) Ab (red) and analyzed by confocal microscopy. (*a*) A ×20 confocal microscopy image of a representative field of amyloid plaques stained with anti-Aβ(3D6) and CTx-B (green) indicating an association of GM1 with developed amyloid plaques in a 12-month $APP_{Sw,Ind}$ mouse brain section. (*Inset*) A ×60 confocal image of an amyloid plaque stained with anti-Aβ(3D6) and CTx-B (green) indicating an association of GM1-positive cells and the amyloid plaque in a 12-month $APP_{Sw,Ind}$ mouse brain section. (*b*) A ×20 confocal microscopy image of amyloid plaques stained with anti-Aβ(3D6) and CTx-B (green) indicating an association of GM1 with developing amyloid plaques in a 9-month $APP_{Sw,Ind}$ mouse brain section. (*c*) A ×20 confocal microscopy image of a field of neurons from an 8-month $APP_{Sw,Ind}$ brain section stained with anti-Aβ(3D6), anti-APP (CT15) (green), and CTx-B (green). Staining indicates polarized CTx-B staining (blue) and colocalized APP (green) and $A\beta_{1-42}$ (red). Arrows (white and yellow) indicate areas of colocalization that are indicated in white by the blending of polarized microdomain staining for CTx-B (blue), APP (green), and $A\beta_{1-42}$ (red) immunoreactivity. Areas of colocalization of APP (green) and Aβ(red) are indicated in yellow by the colocalization of green APP and red $A\beta_{1-42}$. (*Inset*) Control immunocytochemistry by using mouse and rabbit IgG showed no staining. (*d–g*) The ×60 confocal microscopy images of neurons from field panel (*c*) indicate colocalized merge in white (*g*) of APP (*d*, green), $A\beta_{1-42}$ (*e*, red), and CTx-B staining (*f*, blue). (*g*) The yellow arrow indicates polarized soma with internalized CTx-B (blue) and resultant colocalized APP (green) and $A\beta_{1-42}$ (red)/merge yellow. The yellow arrow soma is adjacent to polarized soma with uninternalized CTx-B, suggesting soma at different stages of endocytosis of plasma membrane microdomains. (*h*) A ×60 confocal microscopy image of neurons from $APP_{Sw,Ind}$ mice showing polarized surface-deposited $A\beta_{1-42}$ (red). The arrow indicates polarized soma with surface $A\beta_{1-42}$ (red) and internalized CTx-B (green) colocalized with DAPI (blue). (*i*) A ×60 confocal microscopy image of representative Aβ (red) amyloid-plaque containing GM1-positive cells (Ctx-B, blue) in various degrees of degradation. Ctx-B (green) and DAPI (blue) are colocalized internally in these cells as indicated in white. Similar staining results were obtained with a series of Aβ and APP Abs (listed in *Methods*). The experiments were repeated three times with similar results.

$APP_{Sw,Ind}$ line J9 transgenic mice (C57BL/6 × DBA/2), which express human APP with Swedish (K670N and M671L) and Indiana (V717F) AD mutations and overproduce human Aβ.

Cell Culture. Neuron-enriched cortical cultures were prepared from embryonic day 16 mice as described previously (32). Briefly, ≈4 × 10^5 cells per milliliter were plated on 100-mm plastic culture dishes coated with 100 μg/ml poly-D-lysine, and cultures were maintained in neurobasal medium containing 2% B27 supplement, 2 mM glutamine, 1% penicillin, and 1% streptomycin (Invitrogen) at 37°C in humidified 95% air/5% CO_2. Medium was changed every 3 days, and cells were used for assays after 8–9 days *in vitro*.

Cytochemistry. GM1-enriched membrane lipid rafts were stained with Alexa Fluor 594-conjugated cholera toxin B subunit (Ctx-B; Molecular Probes), mitochondria with MitoFluor Green (Molecular Probes), extracellular amyloid fibrils with thioflavin-S (Sigma–Aldrich), and nuclei with DAPI (Vector Laboratories).

Formalin-fixed human and 4% paraformaldehyde immersion-fixed mouse tissue were paraffin-embedded for immunofluorescence staining. Tissue samples were subjected to HIER by using 10 mM citrate buffer, blocked with 10% donkey serum in PBS, and incubated with mAb Aβ 3D6 (1:100), polyclonal Aβ 10148 (1:50; Abcam), monoclonal Aβ 4G8 (1:50; Abcam), polyclonal Aβ ab5078P (1:100; Chemicon), monoclonal APP 5A31G7

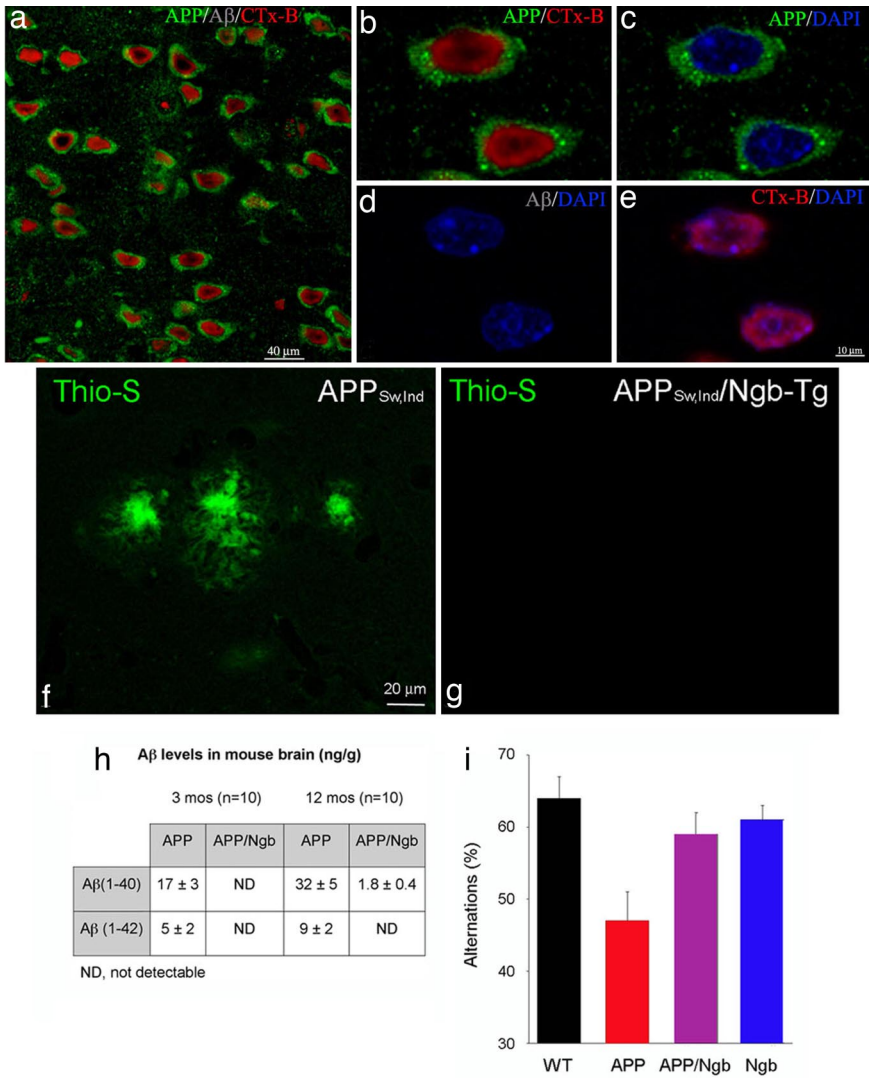

Fig. 4. Somal polarization and $A\beta_{1-42}$ production is inhibited in $Ngb^{++}/APP_{Sw,Ind}$ transgenic mice. Topographical distribution of CTx-B, hAPP, and Aβ as shown by immunocytochemistry in $Ngb^{++}/APP_{Sw,Ind}$ mice brain neurons. $Ngb^{++}/APP_{Sw,Ind}$ 12-month brain sections were stained with CTx-B (red), anti-APP (green), and anti-Aβ Ab (blue) and analyzed by confocal microscopy. (*a*) A ×20 confocal microscopy image of a representative field of neurons from $Ngb^{++}/APP_{Sw,Ind}$ brain indicating decreased plasma membrane CTx-B and increases in nuclear CTx-B staining (red), uniform somal distribution of APP (green), and absence of $A\beta_{1-42}$ (blue). (*b–e*) The ×60 confocal microscopy images of neurons from *a*. (*b* and *d*) Neurons from $Ngb^{++}/APP_{Sw,Ind}$ mice have uniform somal distribution of APP (green), decreased plasma membrane CTx-B, increases in nuclear CTx-B staining (red), and do not make Aβ (gray) (*d*). (*c* and *e*) Uniform somal distribution of APP (green) in $Ngb^{++}/APP_{Sw,Ind}$ mice brain neurons. DAPI-labeled nuclei are in blue. CTx-B (red) colocalizes with DAPI labeled nuclei (blue) (*e*). Control immunocytochemistry by using mouse and rabbit IgG showed no staining. Similar staining results were obtained with a series of Aβ and APP Abs (listed in *Methods*). (*f–i*) Ngb overexpression reduces thioflavin-S staining and Aβ levels and improves cognitive performance in $APP_{Sw,Ind}$ mice. Thioflavin-S staining (green fluorescence) of β-sheet-rich extracellular amyloid fibrils in cerebral cortex of $APP_{Sw,Ind}$ mice (*f*) is diminished in $Ngb^{++}/APP_{Sw,Ind}$ double transgenics (*g*). (*h*) Brains of double transgenic mice also show reduced or absent human Aβ(1–40) and Aβ(1–42) at 3 and 12 months of age. (*i*) Spontaneous alternations in a Y-maze used as a measure of spatial working memory are reduced in $APP_{Sw,Ind}$ mice but restored in $Ngb^{++}/APP_{Sw,Ind}$ double transgenics ($n = 12–15$ per group). Red bar, $P < 0.05$, compared with all other groups (ANOVA and *t* test).

(1:100), or polyclonal intracellular APP CT15 (1:100) diluted in PBS containing 0.1% Triton X-100. The 4°C overnight primary incubation was followed by secondary applications with donkey anti-mouse or rabbit Alexa Fluor 488 (1:250) or 555 (1:500) (Molecular Probes). Images were acquired with a confocal laser imaging system (LSM 510; Carl Zeiss).

***In Vitro* Neurotoxicity.** Lactate dehydrogenase (LDH) release from cortical neurons exposed to 1% Triton X-100-containing lysis buffer was defined as 100% LDH release, and data obtained in other groups were calculated as a percentage of this value. The percentage of nuclei with condensed or fragmented chromatin on DAPI staining or with polarized cell membranes on Ctx-B staining was determined by counting 500 neurons in several random fields. The staining and scoring of all samples was performed in a single-blinded fashion.

Ngb siRNA. The target DNA sequence was ATGGCGCTGCATGTGCGTTGA. Ngb-Tg cortical cultures were pretreated with 4 μM siControl RNA or 4 μM siNgb RNA 24 h before Aβ(25–35) or NMDA treatment. Positively transfected cortical neurons showed decreases in Ngb expression as measured by decreased Ngb immunofluorescence-staining intensity. Transfection of Ngb-Tg cortical cultures with siNgb RNA resulted in 78 ± 12% knockdown of Ngb protein. A similar reduction in Ngb protein levels and results was obtained with Ngb siRNA se-

quence ATGGAGCGCCCGGAGTCAGAG. Images were processed by the Imaris imaging interphase (Bitplane AG). The IsoSurface module was used in Imaris to quantify intensity signals between samples.

Measurement of Aβ. Mouse brain cerebral hemispheres were placed in eight volumes of cold 5 M guanidine HCl/50 mM Tris·HCl (pH 8.0) and homogenized by using a 1-ml Dounce homogenizer. The homogenate was mixed at room temperature for 3–4 h and diluted 1:20 with Dulbecco's PBS containing 5% BSA and 0.03% Tween 20, supplemented with 1× protease inhibitor mixture (4-[2-aminoethyl]benzenesulfonyl fluoride, aprotinin, L-*trans*-3-carboxyoxiran-2-carbonyl-L-leucylagmatine, EDTA, and leupeptin) (Sigma–Aldrich). Supernatants were loaded onto Aβ(1–40) or Aβ(1–42) ELISA plates (Biosource), which were washed four times with wash buffer. Then 100 μl of Aβ standard or sample was loaded into each well and incubated overnight at 4°C. Plates were washed four times, and 100 μl of Aβ(1–40)- or Aβ(1–42)-specific rabbit polyclonal Ab was added. After 2 h at room temperature, plates were again washed four times before 100 μl of secondary Ab (anti-rabbit IgG) was added. After 2 h at room temperature, plates were washed an additional five times, and 100 μl of stabilized chromogen was added. After 30 min in the dark, 100 μl of stop solution was added, and plates were read at 450 nm on a microplate reader. Results were compared with standard curves of synthetic human Aβ(1–40) and Aβ(1–42).

Behavioral Testing. The maze used was a three-arm Y-maze with equal angles between all arms. Each mouse was placed in the center of the Y and allowed to explore freely during an 8-min session. The sequence and total number of arms entered was recorded. Arm entry was considered to be complete when the hind paws of the mouse were completely within the arm. Percentage alternation is the number of triads containing entries into all three arms divided by the maximum possible alternations (the total number of arms entered minus 2) × 100% (33).

Statistical Analysis. Data were analyzed by ANOVA, and post hoc *t* tests with $P < 0.05$ were considered statistically significant.

We thank S. Voglmaier for reviewing the manuscript, M. Khan for discussions, and V. Galvan (Buck Institute) for $APP_{Sw,Ind}$ line J9 mice and 3D6, 5A31G7, and CT15 Abs. This work was supported by National Institutes of Health Grant NS35965 (to D.A.G.).

1. Brunori M, Vallone B (2007) *Cell Mol Life Sci* 64:1259–1268.
2. Khan AA, Wang Y, Sun Y, Mao XO, Xie L, Miles E, Graboski J, Chen S, Ellerby LM, Jin K, Greenberg DA (2006) *Proc Natl Acad Sci USA* 103:17944–17948.
3. Khan AA, Sun Y, Jin K, Mao XO, Chen S, Ellerby LM, Greenberg DA (2007) *Gene* 398:172–176.
4. Fordel E, Thijs L, Martinet W, Lenjou M, Laufs T, Van Bockstaele D, Moens L, Dewilde S (2006) *Neurosci Lett* 410:146–151.
5. Li RC, Pouranfar F, Lee SK, Morris MW, Wang Y, Gozal D (2007) *Neurobiol Aging*, in press.
6. Ehehalt R, Keller P, Haass C, Thiele C, Simons K (2003) *J Cell Biol* 160:113–123.
7. Vetrivel KS, Cheng H, Kim SH, Chen Y, Barnes NY, Parent AT, Sisodia SS, Thinakaran G (2005) *J Biol Chem* 280:25892–25900.
8. Zhou Y, Su Y, Li B, Liu F, Ryder JW, Wu X, Gonzalez-DeWhitt PA, Gelfanova V, Hale JE, May PC, *et al*. (2003) *Science* 302:1215–1217.
9. Desire L, Bourdin J, Loiseau N, Peillon H, Picard V, De Oliveira C, Bachelot F, Leblond B, Taverne T, Beausoleil E, *et al*. (2005) *J Biol Chem* 280:37516–37525.
10. Hsia AY, Masliah E, McConlogue L, Yu GQ, Tatsuno G, Hu K, Kholodenko D, Malenka RC, Nicoll RA, Mucke L (1999) *Proc Natl Acad Sci USA* 96:3228–3233.
11. Bonfoco E, Krainc D, Ankarcrona M, Nicotera P, Lipton SA (1995) *Proc Natl Acad Sci USA* 92:7162–7166.
12. Brown MS, Dana SE, Goldstein JL (1973) *Proc Natl Acad Sci USA* 70:2162–2166.
13. Zacco A, Togo J, Spence K, Ellis A, Lloyd D, Furlong S, Piser T (2003) *J Neurosci* 23:11104–11111.
14. Yanagisawa K, Odaka A, Suzuki N, Ihara Y (1995) *Nat Med* 1:1062–1066.
15. Yamaguchi H, Maat-Schieman ML, van Duinen SG, Prins FA, Neeskens P, Natte R, Roos RA (2000) *J Neuropathol Exp Neurol* 59:723–732.
16. Kawarabayashi T, Shoji M, Younkin LH, Wen-Lang L, Dickson DW, Murakami T, Matsubara E, Abe K, Ashe KH, Younkin SG (2004) *J Neurosci* 24:3801–3809.
17. Sigurdsson EM (2005) *Methods Mol Biol* 299:299–308.
18. Janus C, Chishti MA, Westaway D (2000) *Biochim Biophys Acta* 1502:63–75.
19. Dodart JC, Mathis C, Bales KR, Paul SM (2002) *Genes Brain Behav* 1:142–155.
20. Lalonde R (2002) *Neurosci Biobehav Rev* 26:91–104.
21. Sun Y, Jin K, Mao XO, Zhu Y, Greenberg DA (2001) *Proc Natl Acad Sci USA* 98:15306–15311.
22. Sun Y, Jin K, Mao XO, Zhu Y, Greenberg DA (2003) *Proc Natl Acad Sci USA* 100:3497–3500.
23. Brunori M, Giuffre A, Nienhaus K, Nienhaus GU, Scandurra FM, Vallone B (2005) *Proc Natl Acad Sci USA* 102:8483–8488.
24. Wakasugi K, Nakano T, Morishima I (2003) *J Biol Chem* 278:36505–36512.
25. Schwindinger WF, Robishaw JD (2001) *Oncogene* 20:1653–1660.
26. Wakasugi K, Nakano T, Kitatsuji C, Morishima I (2004) *Biochem Biophys Res Commun* 318:453–460.
27. Kischkel FC, Hellbardt S, Behrmann I, Germer M, Pawlita M, Krammer PH, Peter ME (1995) *EMBO J* 14:5579–5588.
28. Yanagisawa K (2005) *Neuroscientist* 11:250–260.
29. Fassbender K, Simons M, Bergmann C, Stroick M, Lutjohann D, Keller P, Runz H, Kuhl S, Bertsch T, von Bergmann K, *et al*. (2001) *Proc Natl Acad Sci USA* 98:5856–5861.
30. Wang SS, Rymer DL, Good TA (2001) *J Biol Chem* 276:42027–42034.
31. Miida T, Takahashi A, Ikeuchi T (2007) *Pharmacol Ther* 113:378–393.
32. Jin K, Mao XO, Greenberg DA (2006) *J Neurobiol* 66:236–242.
33. Ueno K, Togashi H, Matsumoto M, Ohashi S, Saito H, Yoshioka M (2002) *J Pharmacol Exp Ther* 302:95–100.